AFRL-OSR-VA-TR-2015-0161

S-Layer Based Bio-Imprinting - Synthetic S-Layer Polymers

Dietmar Pum
ZENTRUM FUER NANOBIOTECHNOLOGIE

07/09/2015
Final Report

Air Force Research Laboratory
AF Office Of Scientific Research (AFOSR)/ RTD
Arlington, Virginia 22203
Air Force Materiel Command

REPORT DOCUMENTATION PAGE

Form Approved
OMB No. 0704-0188

1. REPORT DATE *(DD-MM-YYYY)*	2. REPORT TYPE	3. DATES COVERED *(From - To)*
14-07-2015	Final Performance	01-06-2012 to 31-05-2015

4. TITLE AND SUBTITLE
S-Layer Based Bio-Imprinting - Synthetic S-Layer Polymers

5a. CONTRACT NUMBER

5b. GRANT NUMBER
FA9550-12-1-0274

5c. PROGRAM ELEMENT NUMBER

6. AUTHOR(S)
Dietmar Pum

5d. PROJECT NUMBER

5e. TASK NUMBER

5f. WORK UNIT NUMBER

7. PERFORMING ORGANIZATION NAME(S) AND ADDRESS(ES)
ZENTRUM FUER NANOBIOTECHNOLOGIE
GREGOR-MENDEL-STRASSE 33
WIEN, 1180 AT

8. PERFORMING ORGANIZATION REPORT NUMBER

9. SPONSORING/MONITORING AGENCY NAME(S) AND ADDRESS(ES)
AF Office of Scientific Research
875 N. Randolph St. Room 3112
Arlington, VA 22203

10. SPONSOR/MONITOR'S ACRONYM(S)
AFOSR

11. SPONSOR/MONITOR'S REPORT NUMBER(S)

12. DISTRIBUTION/AVAILABILITY STATEMENT
A DISTRIBUTION UNLIMITED: PB Public Release

13. SUPPLEMENTARY NOTES

14. ABSTRACT
The main objective of the proposed work is the development of a key enabling technology for the fabrication of nano patterned thin film imprints by using functional S-layer protein arrays as templates. The unique feature of these imprints is the precisely controlled repetition of surface functional groups and topographical features induced by the crystalline character of the reassembled S-layer protein lattice. The start of the project focused on the selection, composition and chemical modification of suitable polymers (Methacrylic acid (MAA), Vinylpyrrolidone (VP)) as well as on the preparation and reassembly of the S-layer protein SbpA from Lysinibacillus sphaericus CCM2177 on silicon supports that were used as stamps. First of all, the rigidity (expressed by the Young (elastic) modulus) of the S-layer with respect to that of the polymer was investigated in order to make sure that the S-layer is mechanically robust enough to leave an imprint behind. It was found that the Young modulus of the S-layer is ca. 7 times higher compared to that of the polymer.

15. SUBJECT TERMS
Bio-Imprinting

16. SECURITY CLASSIFICATION OF:			17. LIMITATION OF ABSTRACT	18. NUMBER OF PAGES	19a. NAME OF RESPONSIBLE PERSON
a. REPORT	b. ABSTRACT	c. THIS PAGE			Dietmar Pum
U	U	U	UU		19b. TELEPHONE NUMBER *(Include area code)* 43-1-47654-2205

Standard Form 298 (Rev. 8/98)
Prescribed by ANSI Std. Z39.18

Final Report

S-layer based bio-imprinting –

Synthetic S-layer polymers

Agreement Award Nr.: FA9550-12-1-0274

Reporting period: June 1, 2012 to May 31, 2015

Principal Investigator: Dietmar Pum (PI) and Uwe B. Sleytr (Co-PI)

Institution and address: Department of Nanobiotechnology
BOKU - University for Natural Resources and Life Sciences
1190 Vienna, Austria

Reporting date, 6 July 2015

Authors: Dietmar Pum, Eva M. Ladenhauf, and Uwe B. Sleytr

Table of content

Executive Summary

The main objective of the proposed work is the development of a key enabling technology for the fabrication of nano patterned thin film imprints by using functional S-layer protein arrays as templates. The unique feature of these imprints is the precisely controlled repetition of surface functional groups and topographical features – induced by the crystalline character of the reassembled S-layer protein lattice.

The start of the project focused on the selection, composition and chemical modification of suitable polymers (Methacrylic acid (MAA), Vinylpyrrolidone (VP)) as well as on the preparation and reassembly of the S-layer protein SbpA from *Lysinibacillus sphaericus* CCM2177 on silicon supports that were used as stamps. First of all, the rigidity (expressed by the Young (elastic) modulus) of the S-layer with respect to that of the polymer was investigated in order to make sure that the S-layer is mechanically robust enough to leave an imprint behind. It was found that the Young modulus of the S-layer is ca. 7 times higher compared to that of the polymer.

Quartz crystal microbalance (QCM) and Surface Plasmon Resonance (SPR) studies demonstrated outstanding sensitivity and selectivity of the S-layer imprinted sensing layers. The response to rebinding SbpA – the S-layer protein which was used for printing – was linear up to 200 ng / ml protein, and no cross-selectivity to Bovine serum albumin (BSA) or a different S-layer protein (SbsB; *G. stearothermophilus* PV72/p2) was observed.

Based on the successful imprinting of planar surfaces, the molecular imprinting of spherical architectures was investigated too. Micrometer sized liposomes or silica spheres offer the advantage of increased surface areas and consequently a higher number of functional groups or domains. Unfortunately, those experiments did not yield the expected results since liposomes were not stable in DMSO (dimetylsulfoxide) that is used in the polymer synthesis and silica particles were completely enclosed by the polymer and subsequently could not be removed from the imprint. Nevertheless, in the course of theses experiments, S-layer coated bacterial cells (*L. sphaericus* CCM2177) were successfully used as templates. Atomic Force Microscopy (AFM) demonstrated the successful imprinting of the bacterial cells and the attached S-layer lattice.

However, despite the initial assumption, it was not possible to resolve the imprinted S-layer lattice by AFM. We assume that several factors are responsible for this such as plastic deformation at molecular level upon removing the template, water cushions between the S-layer template and the polymer preventing a successful transfer of the S-layer topography into the polymer, or too shallow surface corrugations in relation to the roughness of the polymer. However, Peak Force Quanto Nanomechanical property Mapping (PF-QNM) was able to show that the adhesion of an S-layer coated AFM-tip at the (blank) S-layer imprint was significantly higher than that at the blank reference area.

The use of S-layers as carriers for other molecules and imprinting of the whole assemblies were investigated too. For this purpose, Polycationic ferritin (PCF) (mean diameter ca. 12 nm) was bound in dense packing on the S-layer on the stamp first and subsequently used for generating a square pattern of 12 nm cup-shaped indentations. Successful rebinding of PCF proved that the S-layer lattice can be used as template for making imprints of densely packed and, probably, perfectly oriented biologically functional molecules, a concept that

can in principle be extended to a wide range of other biomolecules (e.g. antibodies, or affinity surfaces) as well as in the material sciences.

In summary, we would like to anticipate that our approach provides a key enabling technology for the fabrication of nano patterned molecular imprints by using self-assembled S-layer lattices. Applications will be found in the life and non-life sciences wherever well defined repetitive topographic and (bio)chemical features in the nanometer range are required.

Part of the work was published already in high-impact journals (8 SCI indexed publ.). Two manuscripts are currently in preparation.

List of publications 2012 – 2015

1. Zafiu, C., Werzer, T., Trettenhahn, G., Pum, D., Sleytr, U.B., Kautek, W. 2014. In Situ Scanning Force Microscopy and In Situ Quartz Microbalance Investigations on the Influence of the Anion Adsorption on the Electrocrystallization of Surface Layer Proteins. J. Phys. Chem. C 118 29860-29865.
2. Pum, D., Sleytr, U.B. 2014. Reassembly of S-layer proteins. Nanotechnology 25:312001.
3. Sleytr, U.B., Schuster, B., Egelseer, E.M., Pum, D. S-layers: Principles and Applications. FEMS Microbiology Review 38:823-864.
4. Prats Mateu, B. Kainz, B., Pum, D., Sleytr, U.B., Toca-Herrera, J.L. 2014. Fluorescent sensors based on bacterial fusion proteins. Methods and Applications in Fluorescence 2:024002
5. Gahleitner, B., Loderer, C., Saracino, C., Pum, D., Fuchs, W. 2014. Chemical foam cleaning as an efficient alternative for flux recovery in ultrafiltration processes. J. Membrane Sci. 450:433-439.
6. Sekot, G. Schuster, D., Messner, P., Pum, D. Peterlik, H., Schäffer, C. SAXS for imaging of S-layers on intact bacteria in the native environment. J. Bacteriol. 195:2408-2414.
7. Pum, D., Toca-Herrera, J.L., Sleytr, U.B. 2013. S-layer protein self-assembly. Int. J. Mol. Sci. 14:2484-2501
8. Schuster, D., Küpcü, S., Belton, D. J., Perry, C. C., Stöger-Pollach, M., Sleytr, U.B., Pum, D., 2013. Construction of silica enhanced S-layer protein cages. Acta Biomaterialia 9:5689-5697

Mansucripts in preparation / submitted

1. Ladenhauf, E.M., Pum, D., Ho, N.P.V, Lieberzeit, P., Sleytr, U.B. 2015. S-layer based biomolecular imprinting. J. Anal. Bioanal. Techn.
2. Ladenhauf, E.M., Sussitz, H., Pum, D., Lieberzeit, P. Characterization of S-layer imprinted polymers by the Peak-Force methods.

PhD Thesis

1. Ladenhauf, E.M. S-layer based bio-imprinting. PhD thesis, BOKU Vienna, 2015.

Statement of objectives

The main objective of the proposed work is the development of a key enabling technology for the fabrication of nano patterned thin film imprints by using functional S-layer protein arrays as templates. Molecular imprinting is a generic technology where compounds with functional groups reciprocal to those of a template are selected for making a scaffold around it. In this way an imprint is formed that is chemically and sterically complementary to the chosen template. Due to the crystalline character of the S-layer template the unique feature of such novel imprints will be the precisely controlled repetition of surface functional groups and domains, and topographical features.

The following specific objectives and tasks have been defined in order to meet the main goals of this project.

	Objectives & Tasks	**Status**
1.	Imprinting of planar S-layer architectures	completed
2.	Imprinting of spherical S-layer architectures	completed
3.	Studying surface properties and phenomena of S-layer imprints	completed
4.	S-layer imprints as patterning elements in Material Science	completed
5.	Double imprinting – Synthetic S-layers	in progress
6.	Exploitation and dissemination of the results	in progress

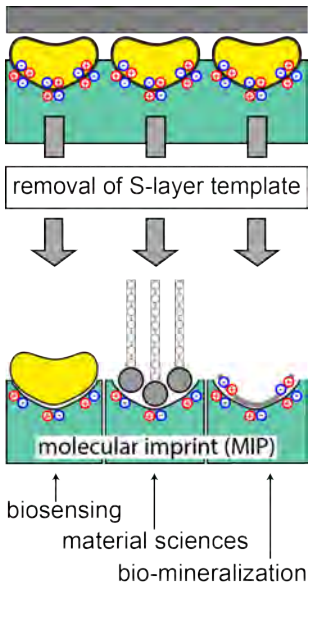

1 Introduction

Molecular imprinting is a well-established technology for generating two- or three-dimensional polymeric matrices for the highly specific detection of chemical or biological analytes [53]. Specificity is obtained by using suitable templates, such as chemical compounds or biomolecules. Self-assembly between these templates and suitable functional groups of the monomers used lead to polymer structures that do not only complement the shape of said species, but also lead to arrangements of functional groups reciprocal to those of the template. Although molecular imprinting was originally developed for detecting and selectively enriching small molecules from liquid matrices by bulk polymer beds [1, 9], extension towards planar sensing layers for larger molecules has attracted substantial attention in the field of biosensor development in recent years [5, 13, 53]. Moreover, planar molecular imprinting mimics the fundamental principle of molecular recognition in nature by offering a bio-analogous surface for binding molecules or antibodies. It is the resulting high sensitivity and selectivity of the imprinted surface towards biomolecules combined with the relatively easy and cheap fabrication which make molecular imprinting to a key option in the development of novel (bio)analytical sensors, separation methods and purification techniques. But, one of the main benefits of a molecularly imprinted sensing layer is the higher robustness of the polymeric material compared to its natural biological counterpart.

Despite all that, it should still be possible to improve the performance of molecularly imprinted surfaces as binding matrices by ensuring perfectly dense packing of, both, topographical features as well as functional groups on the respective template surface. As a matter of fact, in this case the template used for making such high density molecular imprints must be an ordered array of (bio)molecules. In this context, the use of crystalline bacterial surface layer proteins (termed S-layer proteins) seems to be particularly attractive, since S-layer protein lattices have already proven their outstanding properties as affinity and binding matrices in biotechnological and biomedical devices [8, 46, 50].

2 Properties of S-layer proteins

Crystalline bacterial cell surface layer (S-layer) proteins are among the most abundant biopolymers on earth and form the outermost cell envelope component in a broad range of bacteria and archaea (Fig.1.a) [50].

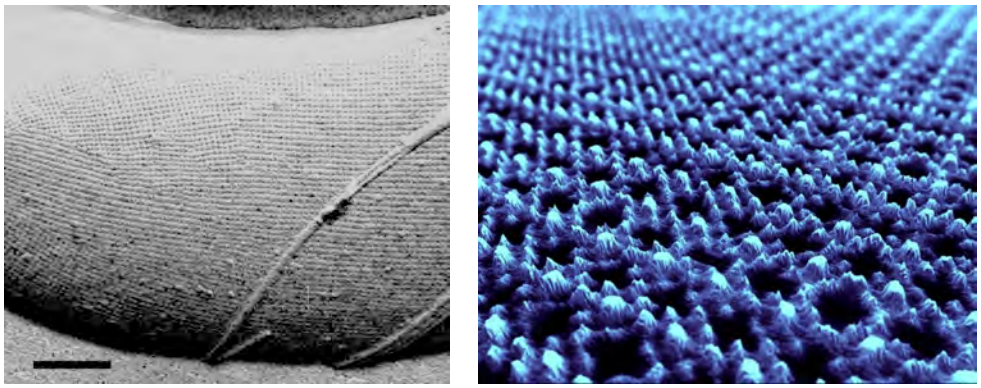

(a) (b)

Fig.1 (a) Transmission Electron Microscopy (TEM) image of a freeze-etched and metal shadowed preparation of a bacterial cell of *Lysinibacillus sphaericus* with an S-layer as the outermost cell envelope component. The S-layer exhibits square (p4) lattice symmetry. The numerous lattice faults are a consequence of the bending of the S-layer lattice at the rounded cell poles. In addition, the rope like structures are the flagella of the bacterial cell. Bar, 200 nm. (b) Perspective view of the SbpA S-layer lattice (from *L. sphaericus*) reassembled on a silicon surface. Image data were obtained by Atomic Force Microscopy (AFM). The size of the unit cell is 13.1 x 13.1 nm.

S-layer lattices consist of a single species of a protein or glyco-protein (M_w 40-200k Da) and may be considered as the simplest biological membranes developed during evolution. They are highly porous protein mesh works with pores of identical size (between 2 and 8 nm) and morphology. S-layers exhibit unit cell sizes of 3 to 30 nm and thicknesses of ca.10 nm. One of the key features of native and genetically modified S-layer proteins, including functionalized S-layer fusion proteins [16, 17], is their natural capability to form self-assembled mono- or double layers in suspension, on solid supports, the air-water interface, planar lipid films, liposomes, nanocapsules, and nanoparticles (for review see [8, 33, 50]) (Fig.1.b).

In this research project, S-layer protein lattices were used for the first time as templates in the fabrication of molecularly imprinted polymer surfaces. The unique feature of these imprints is the precisely controlled periodic repetition of topographical features and surface functional groups – induced by the crystalline character of the S-layer lattice.

3 S-layer proteins used in this project

From preliminary studies and current work we decided to work with the following S-layer proteins:

- SbpA from *Lysinibacillus sphaericus* CCM2177 (square (p4) lattice symmetry; a= 13.1nm, d=8-9nm). [32]
- SbsB from *Geobacillus stearothermophilus* PV72/p2 (oblique (p1) lattice symmetry; a=10.4 nm, b=7.9 nm, γ=81°, d=4.5nm). [31]

The S-layer protein SbpA of the bacterial strain *L. sphaericus* CCM2177 (equivalent to ATCC 4525 [28]) is currently one of the best-characterized S-layer proteins and often used in technological applications [3, 14, 19, 27, 30, 33, 44]. Upon dialysis and addition of Ca^{++} ions [19, 30] SbpA assembles into ordered two-dimensional arrays with square (p4) lattice symmetry in solution and at interfaces, including solid surfaces such as silicon, metals or polymers (for review see [33]). The size of the tetrameric unit cell is 13.1 x 13.1 nm, the thickness in the range of 8 to 9 nm. Calcium ions are mandatory for the reassembly process [30, 31, 36]. SbpA is non-glycosylated and shows a molecular weight of 129 kDa. With respect to the bacterial cell, the outer face is charge neutral due to an equal amount of free amino and carboxyl groups while the inner one is net positively charged due to an excess of amino groups [11].

The SbsB S-layer protein with its molecular weight of 97 kDa is comparable in size to SbpA but reassembles in regular arrays showing oblique (p1) lattice symmetry with lattice parameters of a=10 nm, b=8 nm and a base angle of 81 °. The thickness of the S-layer lattice is approximately 4-5 nm [37, 38]. SbsB is non-glycosylated too. According to SbpA, the outer face is charge neutral but the inner face is net negatively charged due to an excess of free carboxyl groups [37, 38].

Only SbpA S-layer protein lattices were used as templates in the imprinting process since these show pronounced surface corrugations and a thickness of 8-9 nm [14] while SbsB lattices are rather smooth and only 4-5 nm thick [2, 15, 26].

4 Polymer synthesis and spin coating

Polymer synthesis was established in close collaboration with Prof. P. Lieberzeit, Institute of Analytical Chemistry, University of Vienna using standard protocols form previous work [40, 54]. Best results were obtained using methacrylic acid (MAA) and vinylpyrrolidone (VP) in a ratio of 5:2 as functional monomers and dimetylsulfoxide (DMSO) as solvent. N,N'-(1,2-dihydroxyethylene) bisacrylamide (DHEBA) was used as a cross-linker and sodium peroxide sulphate (SPDS) as a radical initiator. After pre-polymerization, the polymer was ready to use (see *Material and Methods* for details).

The polymer was spin coated onto a dual electrode structure (Fig.2) on a 10 MHz quartz crystal microbalance. The thickness was typically in the range of 200 – 300 nm as determined by Quartz Crystal Microbalance (QCM) measurements. In the following, one electrode was imprinted and used as sensing electrode (termed MIP) while the second one was not imprinted and served as (blank) reference (termed NIP). Imprinting was performed overnight at room temperature.

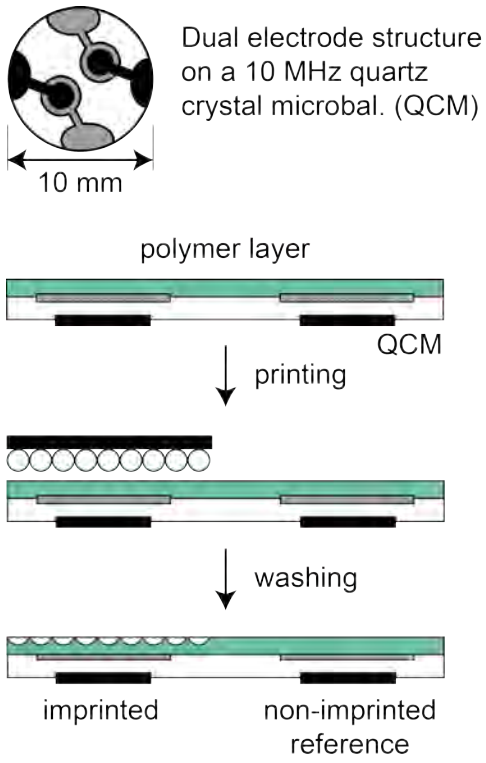

Fig.2 Schematic drawing of the dual electrode structure and the printing process

5 Young modulus of S-layer and polymer at the gel-point

Since the S-layer based imprinting approach is completely new in the field of molecular imprinting, in a first step, we wanted to compare the rigidity (expressed by the Young (elastic) modulus (E)) of the reassembled S-layer protein layer to that of the pre-polymerized oligomer film right after spin-coating (at the gel-point). A higher Young modulus of the S-layer compared to that of the polymer at the gel point is mandatory for a successful transfer of topographical features into the matrix.

In order to determine the Young modulus of the polymer right after spin-coating (at the gel point), force-distance curves were recorded with an AFM in due course (Fig.3).

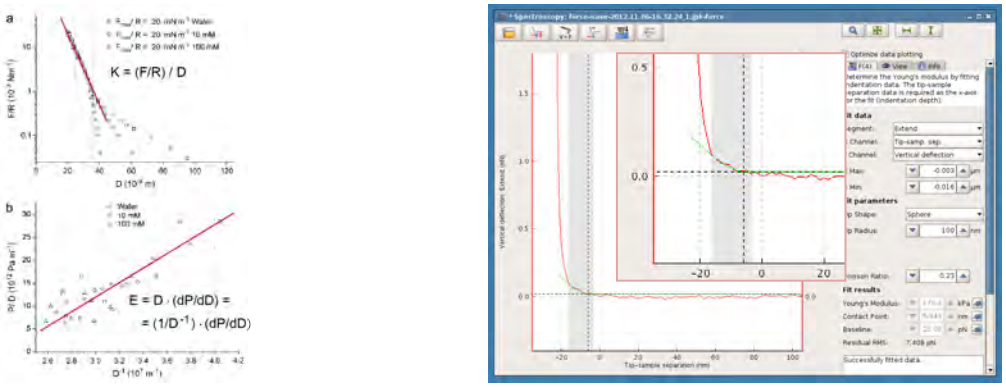

Fig.3 (a) Elastic compression of the S-layer SbpA (*L. sphaericus* CCM2177) based on Derjaguin approximation. The Young modulus (E) as determined with the surface force apparatus is 1.3 MPa. (b) The Young modulus (E) of the polymer (right after spin-coating when the S-layer template is pressed into it) was determined by AFM and found to be 0.17 MPa.

The Young modulus of the pre-polymerized polymer at the gel-point was found to be 0.17 MPa. The Young modulus of the S-layer protein SbpA was known to be 1.31 MPa [23]. The seven to eight times higher Young modulus of the S-layer with respect to that of the polymer led us to the conclusion that it must be possible to transfer the topography and pattern of functional groups of the S-layer protein lattice into the polymer.

6 Characterization of the sensitivity and selectivity of molecular imprints by Quartz Crystal Microbalance (QCM) studies

After removal of the SbpA S-layer functionalized stamp and cleaning the molecularly imprinted (termed MIP) and non-molecularly imprinted (termed NIP) polymer regions,

sensitivity and selectivity of the MIP compared to those of the NIP were determined by exposing both areas to SbpA S-layer protein. QCM studies unambiguously demonstrated the successful rebinding on the electrode surface (Fig.4). Injection of 200 ppm (1 ppm= 1 mg/L) SbpA led to a frequency difference between MIP and NIP in the range of 400 Hz. The baseline refers to water. As shown in Fig.4 the S-layer protein also binds to some extent to the NIP since S-layer proteins bind to polymeric surfaces as well [33] but the MIPs are highly preferred. This experiment was repeated several times with a washing step between each measurement. Moreover, it has to be stressed that the rebinding experiments were carried out without calcium in the solution. Calcium ions are required for the reassembly of SbpA into ordered arrays [30, 31, 36]. The lack of calcium in the subphase guaranteed that only the rebinding of the SbpA proteins was measured and a possible lattice formation at the MIP or NIP avoided.

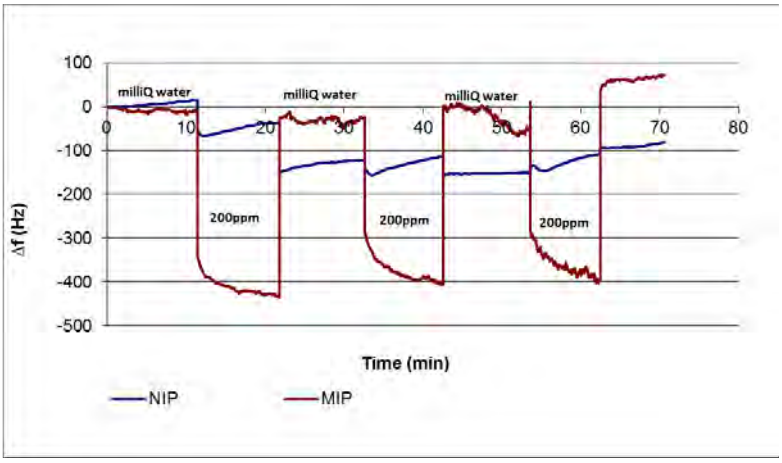

Fig.4 Diagram shows three repeats of rebinding S-layer protein on the molecularly imprinted surface. Measurements were paused during cleaning (injection of SDS-PBS and milliQ water). Baseline refers to water.

In a next step, we determined the QCM sensor characteristic of the S-layer protein MIP and found it to be linear as shown in Fig.5. In the course of these experiments it turned out that the suitable concentration range for rebinding SbpA is 30 to 200 ppm. Above 200 ppm SbpA saturation starts to occur (data not shown).

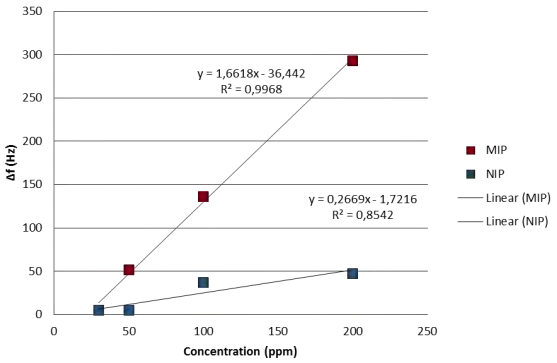

Fig.5 Diagram showing the linear relationship between the QCM frequency response and the S-layer protein concentration in the rebinding experiments.

Selectivity is another important aspect when characterizing a MIP. Therefore we exposed the SbpA MIP and NIP to solutions containing 200ppm of other molecules, such as the SbsB S-layer protein (from *G. stearothermophilus* PV72/p2) as well as Bovine Serum Albumine (BSA) (Fig.6). Both molecules are similar in size to SbpA.

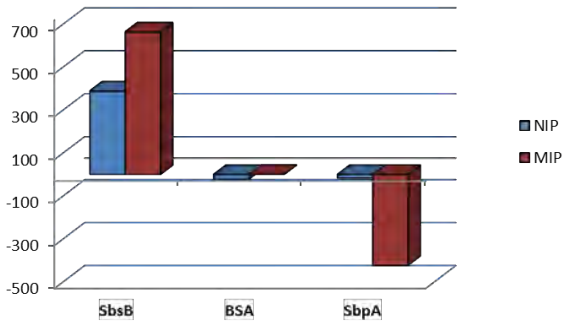

Fig.6 Diagram showing that no cross-selectivity to BSA and even an "Anti-Sauerbrey"- effect upon rebinding of SbsB is observed. As expected SbpA binds preferentially to its own MIP.

While BSA does not lead to a response on the SbpA-MIP, the experiment with SbsB even led to an increase in frequency, a phenomenon that is known as *Anti-Sauerbrey* behaviour. This behaviour has already been observed in other QCM studies with proteins in the literature [21, 40]. An increase in frequency may have been caused by a weak binding of the analyte indicating a low affinity of the target protein to the imprinted surface [6].

7 Characterization of the sensitivity and selectivity of S-layer imprints by Surface Plamon Resonance Spectroscopy (SPR)

Although QCM is the standard method to characterize the binding sensitivity and selectivity of molecular imprints, we had decided to use Surface Plasmon Resonance Spectroscopy (SPR), which is another standard biophysical method, to characterize S-layer based molecular imprints too. For this purpose the same approach as for QCM measurements was chosen (Fig.7.a and b).

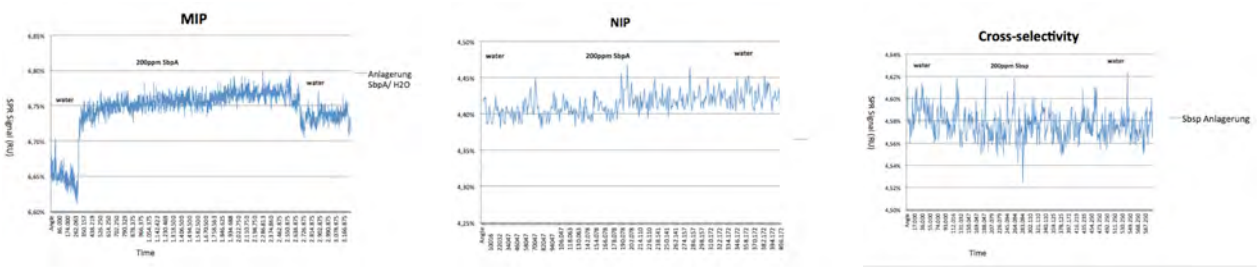

(a) (b) (c)

Fig.7 SPR measurements show (a) the specific rebinding of SbpA S-layer protein at its MIP and (b) no binding to the NIP. (c) No cross selectivity to the SbsB S-layer protein was found.

The SPR measurements showed the specific rebinding of SbpA S-layer protein at its MIP and no binding to the NIP. The high noise level in all measurements was caused by the comparatively high thickness of the spin-coated polymer in comparison to monolayer experiments elsewhere. Moreover, no cross selectivity to SbsB (200 ppm), the S-layer protein from *G. stearothermophilus* PV 72/p2, was found (Fig.7.c). Thus, the use of SPR confirmed the results from the QCM measurements and the fact that the S-layer based imprinting is successful - despite the difficulties in obtaining good AFM images.

8 Improving polymer adhesion on gold electrodes

In the course of the experiments, it was found that upon removal of the stamp the imprinted polymer was partly detached (Fig.8 a). In order to improve the adhesion of the polymer, the gold electrodes were incubated with L-Cysteine prior to the polymer coating. Since this approach led to a considerable improvement (Fig.8b) L-Cysteine coating is part of our standard protocol now.

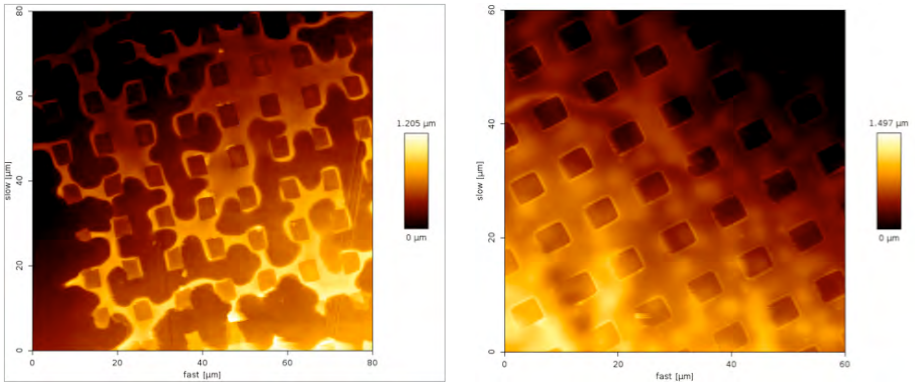

(a) (b)

Fig.8 Molecularly imprinted region after removal a stamp (with a micro lithographically patterned lattice of squares): (a) without L-Cysteine coating, (b) with L-Cysteine coating.

9 Binding of Nile red to S-layer imprints

In another approach, the "charge" imprint of an SbpA S-layer was investigated by binding Nile Red to the imprint. Nile red is an uncharged hydrophobic molecule binding preferentially to polar groups. Nile red was firmly attached to the S-layer imprint and could only be washed off from the non-imprinted reference (Fig.9).

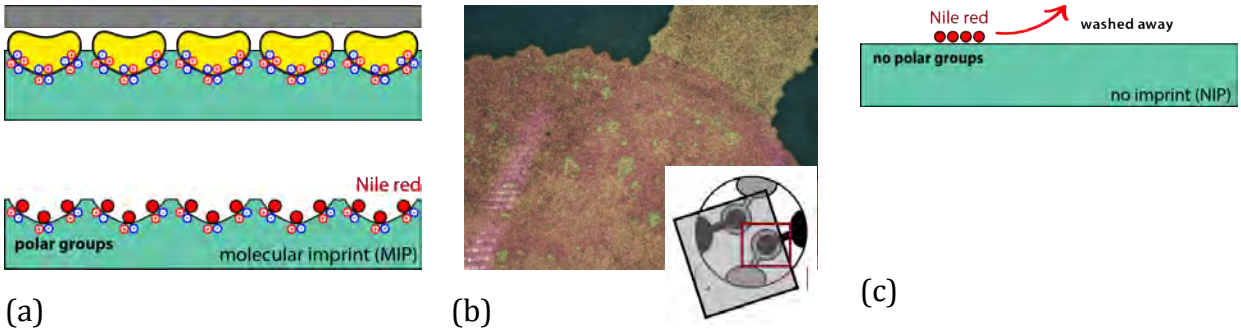

(a) (b) (c)

Fig.9 (a) Schematic drawing showing the formation of polar groups on the S-layer imprint. (b) Fluorescence microscopy image of the Nile red labeled imprint. Inset: The red rectangle shows the image area of the fluorescence image. In order to allow the simultaneous imaging of imprinted (gray square) and non-imprinted regions, the non-contacted area adjacent to the MIP (adjacent to gray square and within red square) was used as reference. (c) Nile red was washed off from the non-imprinted reference electrode.

10 Imprinting of spherical S-layer architectures

According to the project plan, the imprinting of S-layer coated liposomes shall lead to a higher total imprinted surface area and thus to increased signal-to-noise ratios (Fig.10).

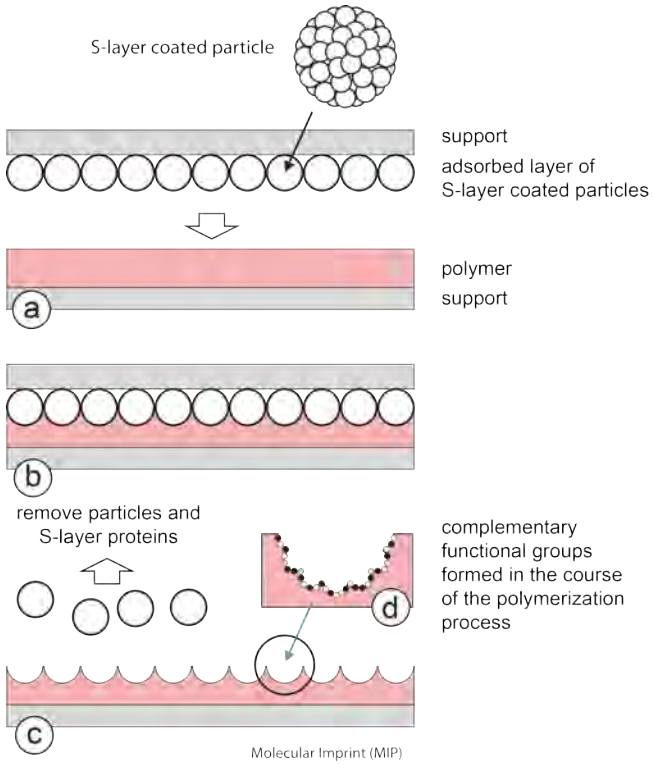

Fig.10 Schematic drawing of imprinting S-layer coated spherical particles

Silica particles

As a preliminary step sc. *Stöber silica particles* were produced since they are mechanically robust and easy to produce in various size ranges. Fig.11 shows Scanning Electron Microscopy (SEM) images of 100 and 500 nm sized *Stöber* particles.

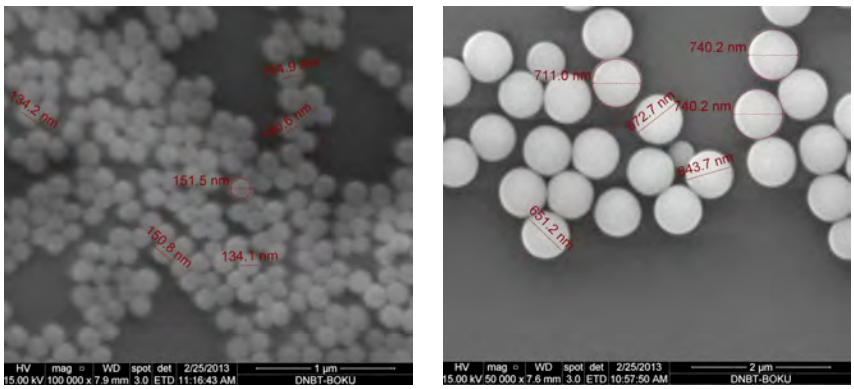

(a) (b)

Fig.11 (a) SEM image of (a) 100 nm, and (b) 500 nm sized *Stöber* particles.

Two approaches were used to coat the *Stöber* particles with S-layer protein and to deposit them on a glass or silicon surface. In the first approach, the *Stöber* particles were silanized with (3-Aminopropyl)triethoxysilane (APTES) in order to improve the adhesion to glass or silicon, deposited as a monolayer on the substrate, and, finally coated with SbpA S-layer protein (Fig.12.a). In the second approach, the *Stöber* particles were coated with an SbpA S-layer first and subsequently deposited as monolayers on glass or silicon (Fig.12.b).

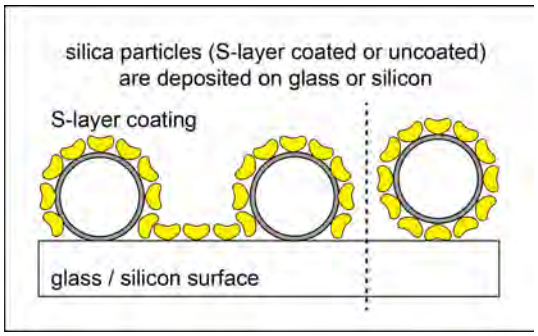

(a) (b)

Fig.12 Schematic drawing of the possibilities to work with S-layer coated *Stöber particles*.

However, although imaging the deposited silica particle monolayers by non-contact AFM was straightforward, it turned out that it is extremely difficult to obtain good AFM images of the S-layer on the silica particles.

Nevertheless, since the S-layer coating of the silica particles followed standard and established protocols (for silica surfaces), it was decided to check the successful S-layer coating by Zeta-Potential measurements.

Three different types of S-layer coated silica particles (500 nm in diameter) were produced and their zeta-potentials determined:

Surface modification	**zeta-potential**
• Silica particles (uncoated as reference)	-82.1 mV
• Silica particles + SbpA	-24.4 mV
• Silica particle + poly-L-lysine (PLL)	40.7 mV
• Silica particle + PLL + SbpA	-31.1 mV
• Silica particle + APTES + SbpA	-31.0 mV

Since a zeta-potential of ca. -30 mV is an established value for a complete S-layer coating, it was concluded that the S-layer coating must have been successful and only the curvature of the silica particles prevented high-resolution AFM imaging. Moreover, it was difficult to remove the *Stöber* particles from the imprints where they were firmly fixed (or submerged) in the polymer.

Liposomes

Due to the described difficulties in using silica particles as scaffolds, it was decided to continue with S-layer coated liposomes. In this way, TEM could also be used to check the individual steps in the course of the preparation procedure. The mono dispersity was determined with a Zeta-Sizer (Fig.13):

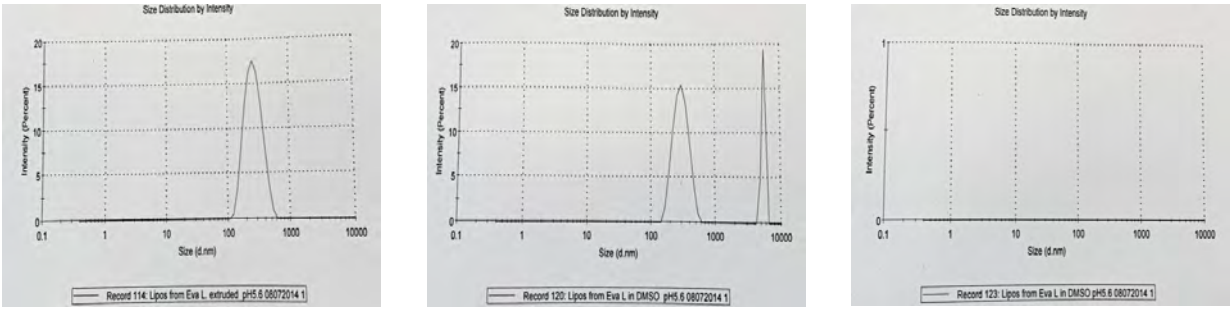

(a) (b) (c)

Fig.13 Measurements show the mono dispersity of (a) liposomes extruded at pH 5,6 (mean dia = 240 +/- 22 nm). (b) Liposomes were immersed in DMSO (pH 5,6) (mean dia = 300 nm), and subequently completely dissolved after 30 seconds as shown in panel (c).

However, it was confirmed that even S-layer coated liposomes are susceptible to Dimethyl sulfoxide (DMSO) that is a key component used in the course of the preparation of the polymer. This observation was confirmed by TEM as shown in Fig.14.

Even crosslinking the liposomes (with glutardialdehyde (GA) or bissulfosuccinimidyl suberate (BS3)) in order to stabilize them did not help. Moreover, S-layer coated (water filled) liposomes were destroyed before a cavity is formed since – it is assumed - DMSO penetrates the pores and dissolves the (inner) lipid shell. As a consequence no complementary groups were formed during the polymerisation process over night.

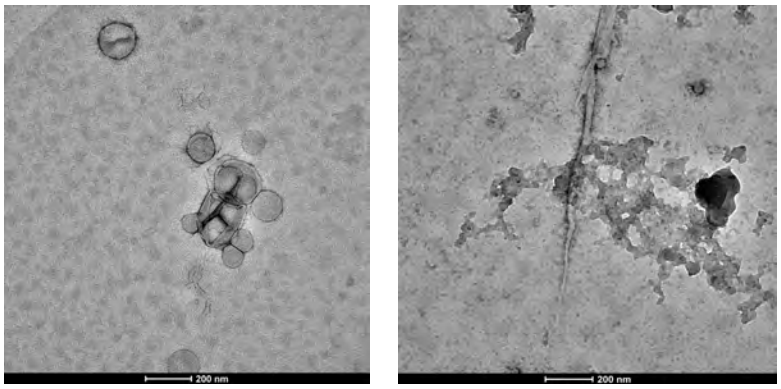

(a) (b)

Fig.14 (a) TEM images of liposomes without DMSO. (b) Liposomes are immediately destroyed after 30 seconds in contact with DSMO.

S-layer coated bacterial cells

Nevertheless, it was found that molecularly resolved imprints of the S-layer lattice could be obtained from wild type bacterial cells from *L. sphaericus* CCM2177 showing the SbpA S-layer protein lattice as the outermost cell envelope component (Fig.15.a and b).

In the course of the experiments it was found that the bacterial cells were pressed too deep into the polymer using the standard imprinting protocol (Polymer: MAA-VP, no delay upon imprinting). Thus the pre-polymerization time was increased leading to an increased stiffness, which was sufficient for successful imprinting. AFM demonstrated the successful imprinting of *L. sphaericus* CCM2177 cells (Fig.15.c). However, this modification in the printing process led to no improvement in the imprinting of liposomes.

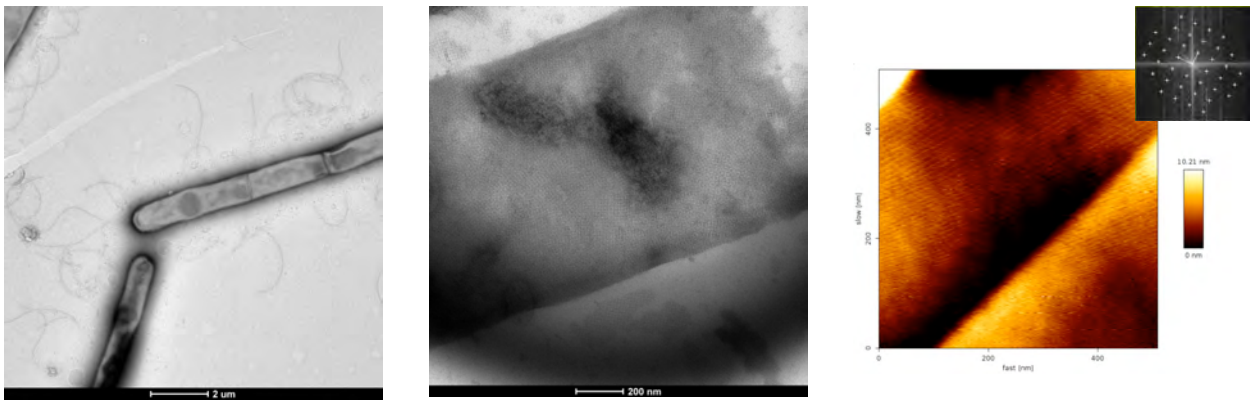

(a) (b) (c)

Fig.15 (a) and (b) TEM micrographs showing *L. sphaericus* CCM2177 cells. (c) AFM micrographs showing the imprints of *L. sphaericus* CCM2177 cells. The inset shows the digital Fourier transform of the AFM image. The reciprocal lattice points (indicating the square lattice symmetry) are marked by crosses and the base vector pair indicated by arrows.

11 Imaging S-layer imprints by Atomic Force Microscopy (AFM)

High resolution AFM imaging of reassembled S-layer protein lattices is routinely applied in the investigation of S-layers in our group. For example, Fig.16 shows an AFM image of SbpA reassembled into an ordered two-dimensional crystalline lattice with square (p4) lattice symmetry at the surface of the stamp. Unit cell size is 13.1 x 13.1 nm.

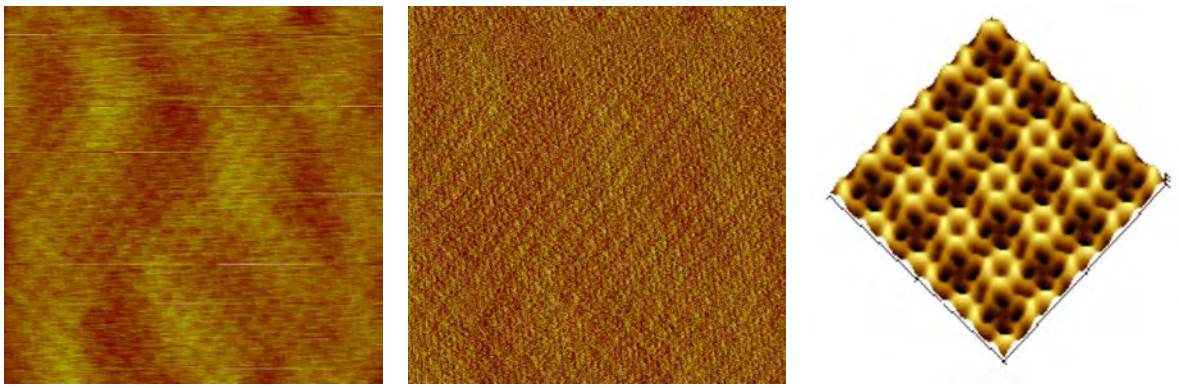

(a) (b)

Fig.16 (a) AFM image (contact mode in liquid) of an SbpA monolayer on a silicon wafer used for stamping. Height image (left; z-range 3 nm), deflection error image (right; z-range 0.3 nm), image size 600 x 600 nm. (b) Perspective view on the inner face of the SbpA S-layer after using image processing techniques to enhance the signal to noise ratio. The unit cell size of the S-layer lattice is 13.1 x 13.1 nm.

However, despite the initial assumption that the polymeric imprints of S-layer lattices may also be easily visualized by AFM, neither contact- nor non-contact mode AFM was able to resolve the imprinted structure(s).

We assume that several factors are responsible:

1. Plastic deformation of the imprint may occur when the template is removed, although extreme care was taken. It is well known now for several decades that plastic deformation at molecular level also occurs at extreme cryogenic temperatures (4K) [45, 47, 48, 51].
2. Inspection of spin-coated polymer layers by AFM yielded a mean roughness of up to 200 to 300 nm which is by far too much for imaging S-layers with mean corrugations in the nanometer range. For SbpA, the mean depth of the S-layer protein induced cavities is approximately 3 to 4 nm. Thus, the signal level compared to the background variation is only in the 1% range. Although, in the synthesis protocol the

complete substitution of water by Dimethyl sulfoxide (DMSO; $(CH_3)_2SO$)) led to a smoother surface roughness of the polymer, the overall difficulty of obtaining smooth polymer layers over the entire sensor surface area remained.

The difficult and time consuming task of finding suitable S-layer patterns in the corrugated polymer surface could be mitigated by using lithographically patterned stamps. A silicon wafer with a micro lithographically fabricated pattern of squares (3 – 6 µm width, 700 nm depth) was introduced as novel support for the S-layer (Fig.17).

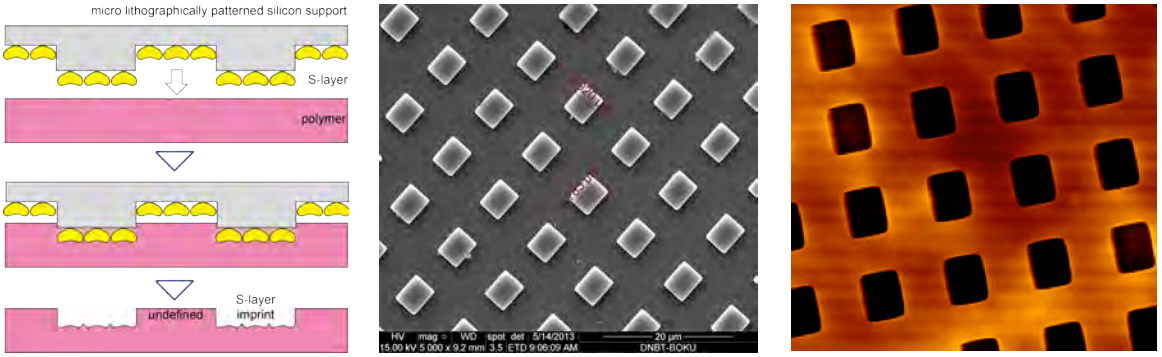

Fig.17 (a) Schematic drawing of a cross-section through the patterned mask. (b) SEM image of the stamp, and (c) AFM image of the polymeric imprint.

3. Moreover, in case the polymer does not absorb the residual water contained in the pores and cavities of the S-layer protein lattice, a "deep" imprint of the S-layer in the polymer will not be possible since the S-layer will be squeezed by the water film and just the upper part of the protein lattice may contribute to the imprint. This hypothesis was supported by the observation that QCM data could not be obtained from the same polymer composition when water was used as solvent instead of DMSO. DMSO is miscible with water (and alcohols, acetone, chloroform and benzol) and thus it takes-up a certain amount of residual water set free in the course of the polymerization.

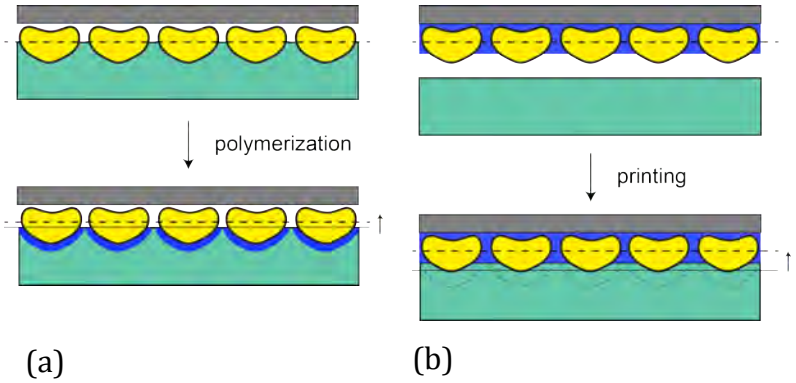

Fig.18 Schematic drawings of (a) water set free in the course of the polymerization leading to a floating of the supported S-layer, and (b) residual water (particularly) in the S-layer pores.

4. Moreover, it was found that the polymer was swelling in liquid (milliQ water) within 20 min. In this experiment, 200 nm sized silica particles were used as template for imprinting the polymer. Then, the imprint was immersed in water and the diameter of a cavity determined at consecutive time intervals by AFM: After 1 hour the diameter of the originally 193 nm sized imprint was 292 nm (51 % increase), and after 2 hours 381 nm (97% increase). But, high resolution AFM usually requires imaging in buffer in order to minimize the loading forces, in particular electrostatic interactions between tip and surface. However, AFM in air was used too in order to avoid the negative swelling effect but molecularly resolved S-layer structures could not be obtained either.

12 S-layer imprints as patterning elements in material sciences

One of the major goals in this project was the combination of the self-assembly properties of S-layers as materialized in mechanically robust S-layer-MIPs with functional materials, such as metallic nanoparticles. As shown schematically in Fig.19, nanoparticles may be either synthesized in wet chemical approaches [43] or by Physical Laser Deposition (PLD) or, alternatively, produced in solution and bound as preformed particles [11] . Another approach would involve the silicification of the surface with biogenic silica [10, 42].

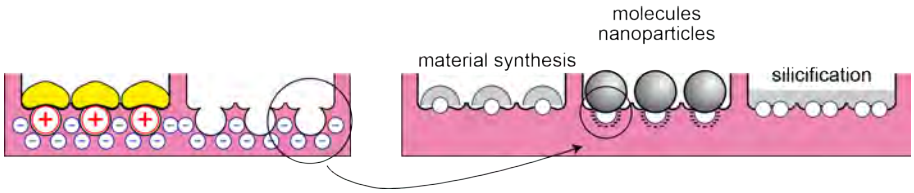

Fig.19 Schematic drawing in using S-layer imprints as patterning elements in material sciences.

In the first attempts concerning the binding, printing, and re-binding of molecules, polycationic ferritin (PCF) was used as model system. Polycationic ferritin (PCF) is a ferritin molecule cationized by N,N-dimethyl-1,3-propanediamine (DMPA) with amino groups. PCF is a well-known marker molecule in TEM since the iron core yields high contrast and the positive charge allows the labeling of negatively charged groups, such as carboxyl groups, for example on proteins [24, 29]. PCF has a mean diameter of 12 nm, and thus is perfectly suited to label S-layer unit cells individually. The binding of PCF onto the S-layer and the subsequent molecular imprinting was done in order to show that it is possible to use the S-layer itself as a "stencil" for (bio)molecules, i.e to achieve optimal assembly, and to answer the question if the MIP still preferably rebinds PCF because the NIP offers free carboxyl groups on its surface too. In detail, does the imprinting of the positively charged PCF lead to a noticeable re-distribution of the carboxyl groups in the pre-polymer into clusters of negative charge in addition to the topographical effect of a nano metric "egg carton" with hemi-spherical indentations in the 12 nm range.

As a first step, SbpA S-layer protein was reassembled as a monolayer on a patterned silicon wafer (rendered hydrophilic by plasma treatment). Subsequently, the amine groups (NH_3) groups were cross-linked with 2,5% glutardialdehyde leading to a net negative surface charge. Then, PCF (10 mg/ml) was bound to the S-layer pattern (Fig.20).

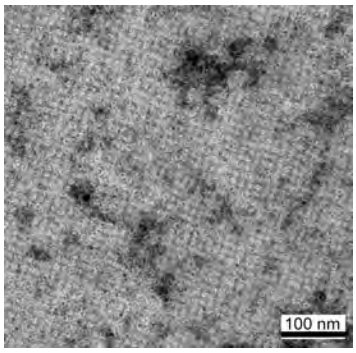

Fig.20 TEM of PCF bound to an SbpA S-layer monolayer.

The rebinding of 200 ppm PCF led to an average frequency decrease of 450 Hz at the MIP and of 350 Hz at the NIP corresponding to a usable sensor signal of 100 Hz (Fig.21a).

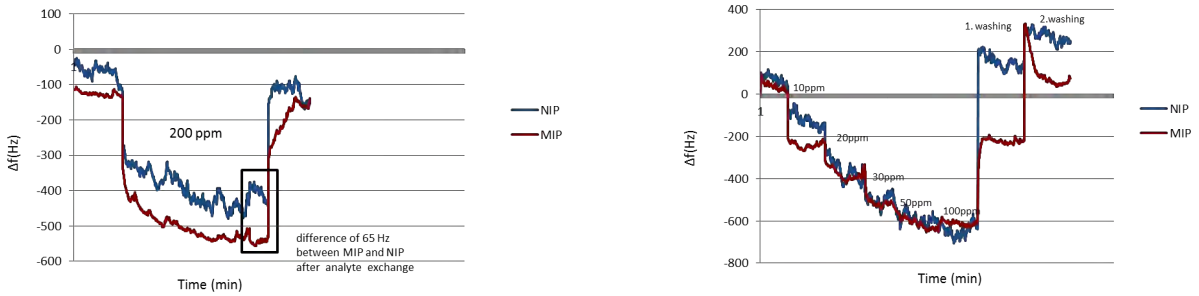

(a) (b)

Fig.21 Diagram showing (a) the rebinding of PCF 200 ppm on imprinted (magenta) and non-imprinted (blue) electrode surfaces. (b) PCF bound to the imprinted surfaces withstands the washing with SDS-PBS much better than that on the non-imprinted area. Baselines refer to water.

According to the investigation with the SbpA S-layer protein, the maximum amount of PCF that can be rebound to the imprinted area was determined too (Fig.21b). After addition of 10 ppm PCF, the frequency at the MIP decreased by 300 Hz while at the NIP by 200 Hz. After further additions of PCF leading to a (final) concentration of 50 ppm PCF in the analyte an increase to 100 ppm PCF did not lead to a further frequency decrease. Thus, it was concluded that the saturation condition at the imprinted electrode surface must be in the range of 50 to 60 ppm.

The positive effect of molecular imprinting for binding PCF could be demonstrated by washing the two PCF loaded sensor surfaces in two consecutive steps (Fig.21b). After the first washing step (10 min with 0.01 % SDS, PBS, and milliQ water, respectively) the electrode signal at the NIP reached the baseline again whereas the signal of the MIP did not change as much. In a second washing step (now 15 min) PCF, which was still bound to the imprinted surface, was removed as well. Moreover, the exchange of the analyte solution with water (shown as boxed area in Fig. 20a) caused a slight increase of the frequency of 65 Hz on the NIP electrode but none on the MIP. These results confirm a higher affinity of the PCF to the MIP compared to the NIP.

13 Peak-Force Quantitative Nanomechanical property Mapping

Peak-Force Quantitative Nanomechanical property Mapping (PF-QNM)[1] was used to demonstrate the different adhesion forces at MIPs and NIPs by …

- Mapping rebound S-layer protein with a blank tip (Fig.21.a and b), and
- Mapping the blank regions with a functionalized tip (Fig.21.c and d).

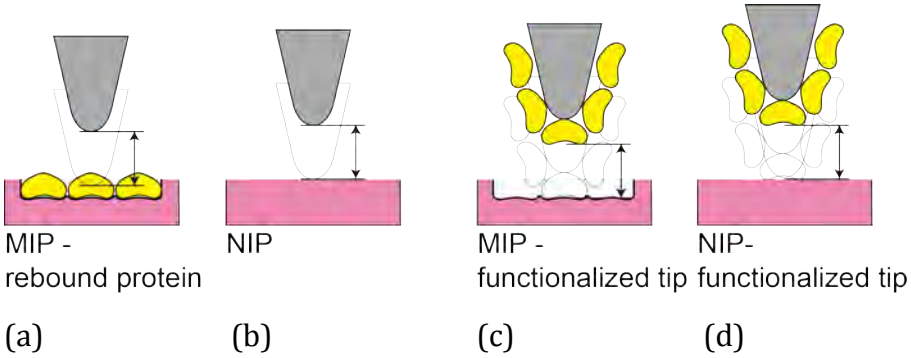

Fig.21 Schematic drawings of mapping the different adhesions of (a) S-layer protein rebound at a MIP, (b) a non-imprinted region, and (c) a functionalized tip on a blank MIP, and (d) on a blank NIP.

Mapping with a blank tip

As a consequence of the difficulties in direct imaging of the S-layer imprints by AFM, we decided to use PF-QNM to demonstrate that S-layer protein is specifically and firmly attached to the MIP surface by determining the adhesion of a blank tip to the MIP in comparison to the NIP after thorough washing (Fig.21.a and b).

The statistical analysis of the adhesion forces on the molecularly and non-molecularly imprinted areas is summarized in Fig.22. The diagram shows that the adhesion forces are comparable for the blank MIP and NIP surfaces while a significant increase is observed for the MIP with rebound S-layer protein after washing (0,1% SDS, 10mM PBS pH 7,4 and milliQ water in consecutive steps).

---

[1] Bede Pittenger, N.E., Chanmin Su, Quantitative Mechanical Property Mapping at the Nanoscale with PeakForce QNM.
In Vecco: http://www.veeco.com/pdfs/appnotes/Quantitative-Mechanical-Property-Mapping-at-the-Nanoscale-with-PeakForce-QNM-AN128-LoRes.pdf.

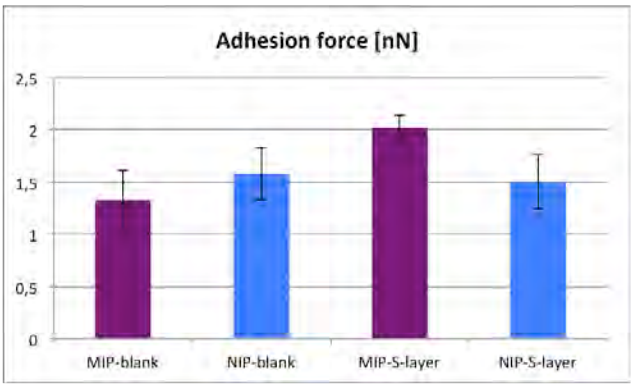

Fig.22 Diagram summarizing the mean value and standard deviation of the adhesion forces between a (blank) tip and the blank MIP and NIP, as well as for the functionalized MIP and NIP after thorough washing.

Although it is not possible to visualize the S-layer lattice by PF-QNM (Fig.23), the measurements clearly confirmed the results from the QCM studies. In order to facilitate a direct comparison between the MIP and NIP, the same z-scale for the adhesion force (2.0 nN full scale) was used in all images in Fig.23. Since the adhesion of the blank tip to a blank surface is very low, panel (a) and (c) look very dark. But the adhesion of the tip to the rebound S-layer protein becomes visible in (b) while the adhesion to the non-imprinted electrode (d) remains low. The images in (b) and (d) were taken after 2 hours of incubation of the MIP and NIP, respectively, with S-layer protein. However, a little amount of protein is bound to the NIP too. The measurements were carried out in air.

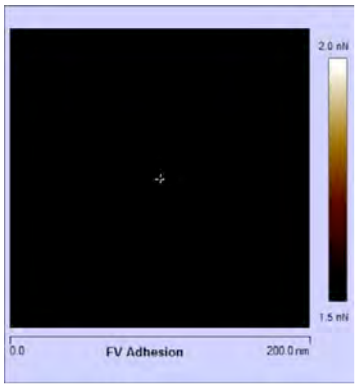

(a)

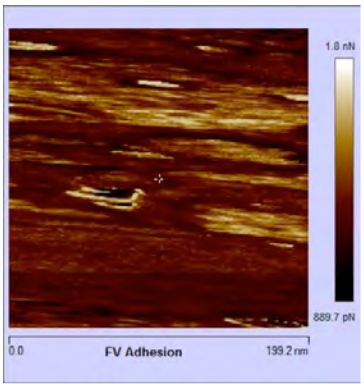

(b)

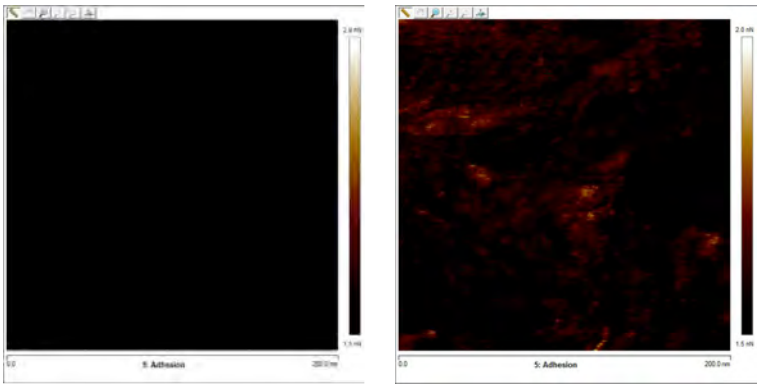

(c) (d)

Fig.23 Peak Force QNM with a blank tip of (a) a blank MIP, (b) S-layer protein rebound to the MIP (after 2 hours), (c) blank NIP, and (d) NIP where a small amount of S-layer protein was bound as well (after 2 hours).

Mapping with an S-layer functionalized tip

While the determination of the adhesion of a blank tip to an S-layer coated surface was more a replacement of the direct AFM-imaging, the mapping of the MIP and NIP with an S-layer functionalized tip closely resembles the molecular recognition process between the S-layer and the MIP associated with a strong binding to the surface. As a consequence, the measurements were carried out in liquid resulting in much lower adhesion forces compared to the measurements performed in air (described before). In Fig.24 the statistical analysis of the mean adhesion value (and the standard deviation) is summarized. As expected, the adhesion force of the S-layer coated tip is approximately three times higher (mean value of 191.57 pN) on the MIP compared to the NIP (mean value of 72.99 pN). For comparison, the same mapping experiment was carried out with a blank tip on the blank MIP and NIP too. In both cases, the adhesion between the blank MIP and NIP and the blank tip was the same (mean value of 212.10 pN at the MIP and 217.47 at the NIP). It is surprising that the results from the blank tip are higher than those from the S-layer coated tips but may be interpreted in the view of the antifouling properties of S-layers. Work will be continued to clarify this observation unambiguously.

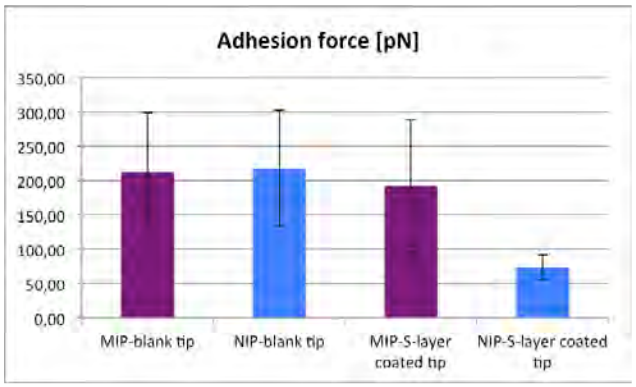

Fig.24 Diagram summarizing the mean value and standard deviation of the adhesion forces between the blank tip and the MIP and NIP, as well as for the S-layer coated tip and the MIP and NIP after thorough washing.

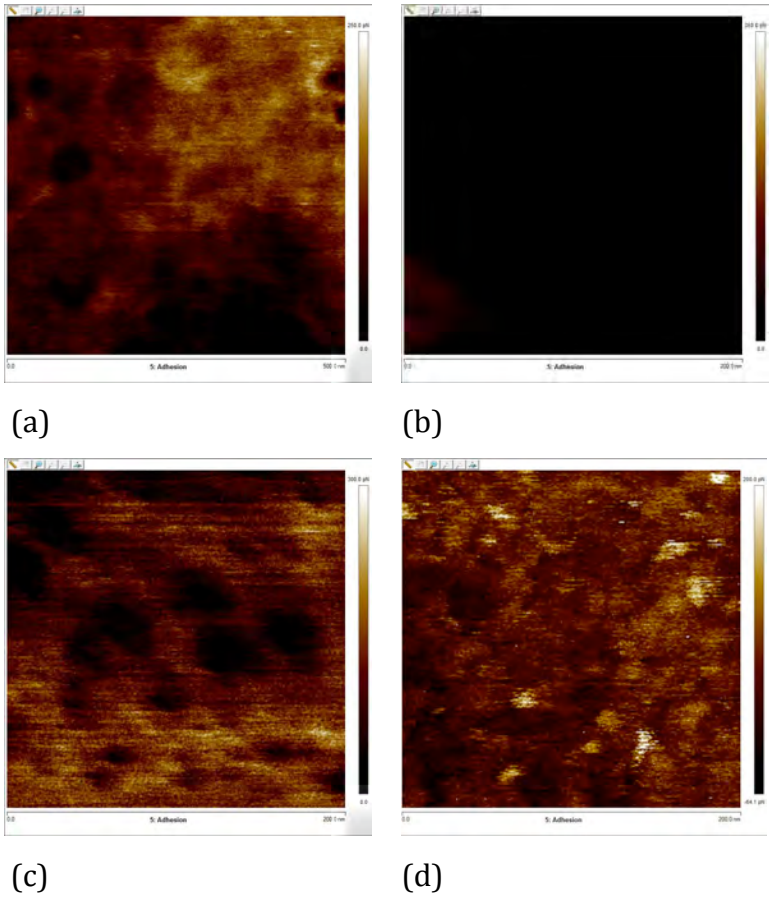

Fig.25 PF-QNM with a blank tip of (a) a blank MIP, (b) blank NIP, as well as for an S-layer coated tip of (c) a blank MIP and (d) a blank NIP.

14 Imprinting the imprints

According to the proposed project plan we tried to make an imprint of the imprint in order to get a synthetic copy of the S-layer used as template in the molecular imprinting process. However, although theoretically possible, it turned out that the two polymers were sticking firmly together in the course of the casting process and could not be separated without destroying them. Thus it was decided to postpone this task to a later date.

15 Conclusions from the project – Impact on the field

The use of S-layer protein lattices is completely new in the field of molecular imprinting. It is the two-dimensional lattice, which make this approach so unique, because up to our knowledge, there is no other biological model system available which provides such a precisely controlled spatial distribution and orientation of physicochemical properties in the nano meter range. This feature of S-layer protein lattices has already been widely used in nanobiotechnological applications where molecules or nano particles were bound into regular arrays such as in the development of high density affinity matrices [8, 17, 26, 46, 50, 52].

In the course of the project it was possible to demonstrate that S-layers may be used as templates in molecular imprinting and the resulting imprints are highly sensitive and selective sensing layers. The whole process including the synthesis and spin coating of the polymers, the S-layer reassembly and the characterization of the imprints by QCM are well established now. However, imaging the molecular structure of the imprints by AFM was not possible. We think that several factors are responsible although the plastic deformation of the polymeric imprint upon removal of the stamp might be the most severe one. Nevertheless, QCM, SPR and PF-QNM clearly demonstrated the functionality of the molecular imprints. Thus we concluded that in addition to the topography of the imprints the distribution of charges - complementary to the functional groups on the S-layer - play an important role in the molecular recognition upon binding of the same or different molecules.

Moreover, with the design and expression of functional S-layer fusion proteins, a new horizon in biotechnological and biomedical research was opened since then it was possible to specifically functionalize the S-layer proteins and thus the entire reassembled S-layer lattice. In this way, the molecular imprinting of S-layer proteins may become extremely valuable when functional domains such as streptavidin or metal precipitating peptides are fused with the S-layer proteins and imprinted into the polymeric surface. The proof-of-principle for this fundamental concept was shown here by binding PCF to the S-layer protein template in dense packing, imprinting the PCF array, and, after washing, rebinding PCF. Although the S-layer will only serve as a template and together with the functional layer sacrificed after the imprinting process, the molecularly imprinted sensing layer will be mechanically much more robust than its natural counterpart. Moreover, it might be possible but also extremely challenging to make a functional imprint of the imprint and in this way a "synthetic copy" of the topography and surface functional groups (or domains) of the original S-layer lattice. This approach was tried already in the course of this project but would require much more time to be successfully completed. However, it would be a contribution to the rapidly growing area of synthetic biology, too. Moreover, a broad range of S-layer protein is glycosylated [25, 41, 50]. The carbohydrate chains are located at the outer S-layer face and – when the S-layer protein reassembles with its inner face at the stamp surface - thus accessible for molecular imprinting too. It would be interesting to see whether it is possible to bind and align carbohydrate chains in a precisely controlled way on a polymeric surface.

In summary, we would like to anticipate that our approach provides a key enabling technology for the fabrication of nano patterned molecular imprints by using self-assembling strategies common in nature. Application will be found in the life and non-life sciences wherever well defined repetitive topographic and (bio)chemical features in the nanometer range are required.

16 Acknowledgements

The support of Peter Lieberzeit, University of Vienna, Institute of Analytical Chemistry, Vienna in establishing the molecular imprinting process is gratefully acknowledged.

We would like to thank the AirForce Office of Scientific Research (AFOSR) for funding this project !

17 Material and Methods

Bacterial strains, growth conditions, cell wall preparations, and S-layer protein isolation

The S-layer proteins, SbpA from *Lysinibacillus sphaericus* CCM2177 [19, 30] and SbsB from *Geobacillus stearothermophilus* PV72/p2 [2, 39], were used in this work.

L. sphaericus CCM2177 was grown in continuous culture nutrient broth medium under carbon limitation at 30°C [19, 30] and *G. stearothermophilus* PV72/p2 in SVIII medium at 57°C. Both organisms were harvested from the growth medium by centrifugation (at 10,000 g). Cell wall preparations of both S-layer proteins followed the procedures described in [49].

S-layer proteins were isolated from cell wall preparations by extraction with 5 M guanidine hydrochloride (GHCl; Fluka, Buchs, Switzerland) according to a previously described procedure [49]. The supernatant containing the proteins was dialyzed against 10 mM $CaCl_2$ (for SbpA) or milliQ water (for SbsB), respectively, as described previously [7, 18, 49].

Polymer synthesis and spin coating

Polymers were synthesized following protocols published in previous work [40, 54]. Best results were obtained using methacrylic acid (MAA) and vinylpyrrolidone (VP) in a ratio of 5:2 as functional monomers and dimetylsulfoxide (DMSO) as solvent. N,N'-(1,2-dihydroxyethylene) bisacrylamide (DHEBA) was used as a cross-linker and sodium peroxide sulphate (SPDS) as a radical initiator. After pre-polymerisation the polymer was ready to use.

Stamp preparation

Silicon wafers were cut in 5 x 5 mm pads and pre-cleaned with 70 % ethanol and milliQ water. Very clean hydrophilic silicon surfaces were obtained after O_2 plasma treatment (20 s at 0.01 mbar) (Model Plasma Prep II, Gala Instruments, Germany). Subsequently, the

silicon pads were placed on the surface of an S-layer protein solution (0.1 mg/ ml SbpA in 0.5 mm Tris-HCl buffer, pH 9, 10 mM $CaCl_2$, RT) in a beaker. The S-layer protein reassembled on the silicon surface and formed monolayers over night [12, 33, 34].

For binding of polycationic ferritin (PCF) the reassembled S-layer proteins were treated with 2.5 % glutaraldehyde in 0.1 M Cacodylate buffer (pH 7.2) for 20 min to crosslink the amino groups. After washing with milliQ water for 5 min, PCF (Sigma life science; 10 mg/ mL) was bound to the free carboxyl groups (incubation time 10 min) [4, 24, 29].

Sensor fabrication and Quartz Crystal Microbalance (QCM) measurement

Dual-electrode sensor geometries were screen-printed on AT-cut quartz discs (10 MHz, 15.5 mm in diameter) with a brilliant gold paste (Heraeus, Germany) and baked for 2 hrs at 400°C as published previously [6]. The quartz discs with the dual electrode configuration were spin-coated with the pre-polymerized polymer subsequently. Thickness was typically in the range of 200 – 300 nm as determined by QCM measurements. In the following, one electrode was imprinted and used as sensing electrode while the second one was not imprinted and served as (blank) reference. Imprinting was performed overnight at room temperature using the SbpA S-layer protein coated silicon pads as stamps. After careful removal of the stamp, the polymer coated quartz discs were placed in milliQ water for 5 hr and washed with 0,1 % sodium dodecyl sulfate (SDS), phosphate buffered saline (PBS) (10 mM, pH 7.4) and milliQ water in order to remove residual SbpA protein.

Sensors were investigated with a network analyser (Agilent 8712ETA, Agilent Santa Clara, CA) in a measuring cell made of poly(dimethyl-siloxane) (PDMS; volume of 125 µL) at RT in liquid. In the course of the measurements the analyte was injected into the cell and the mass uptake recorded for 7 min. In the following, between each measurement cycle, the measurement was paused and the sensor surface (imprinted and non-imprinted area) was washed for 15 min with 0.1 % SDS, PBS (10 mM, pH 7.4) and milliQ water in consecutive steps.

Determination of the Young modulus of the pre-polymerized polymer

In order to determine the Young modulus of the polymer right after spin-coating (gel point), force-distance curves were recorded with an AFM in due course. The Young modulus was

calculated by the AFM software. A spherical tip with a radius of 100 nm (determined by SEM) and a Poisson ratio of 0.23 was assumed for the fitting procedure.

Nile red (9-diethylamino-5H-benzo[α]phenoxazine-5-one) staining

Prior to Nile red (NR) staining, the sensor surfaces were incubated in 8 M urea, followed by cleaning with 0.1 % SDS (15 min) and 10 mM PBS (pH 7.4) (15 min), and rinsing in milliQ water in order to remove residual protein from the printing process. After treatment with 10 µM NR (in 10 mM PBS (pH 7.4)) for 15 min, the sensor surfaces were washed with milliQ water again. Subsequently, the devices were treated with 10 µM NR (in 10 mM PBS (pH 7.4)) for 15 min a second time, followed by final rinsing in milliQ water. Images were recorded using a fluorescence light microscope (Eclipse LV100; Nikon, Tokio, Japan).

Preparation of Stöber particles

In the sc. *Stöber* process, tetraethyl silicate is added to an excess of water containing a low molar-mass alcohol, such as ethanol, and containing ammonia. After stirring, the resulting silica particles have diameters between 50 and 2000 nanometers depending on the type of the silicate ester used, type of alcohol used, volume ratios (in particular ammonia), temperature and time (see Table 1)

Table 1: Overview of the parameters used to make Stöber particles

particles size	ammonia 33%	TEOS	H_2O	ethanol 99%	time / temp.
100nm	1,597ml	6,245ml	15,12ml	93,75ml	3h/RT
500nm	6ml	6,245ml	15,12ml	93,75ml	3h/RT

Liposomes

A slightly modified liposome preparation method to that described by Kirby and Gregoriadis [20] was used to produce positively charged liposomes. The lipid mixture consisted of dipalmitoylphosphatidylcholine (DPPC; Avanti Polar Lipids, Alabaster, AL, USA), cholesterol (Sigma, St. Louis, MO, USA) and stearylamine (Fluka, Buchs, Switzerland) in a molar ratio of 10:5:4. Due to the HDA in the lipid composition, the liposomes have a positive surface charge that favors the reassembly of the S-layer protein, similar to bacterial

cells. A lipid stock solution containing 30 mg • ml^{-1} DPPC was prepared by dissolving all of the lipids in 2 ml chloroform and rotary evaporated at 60°C under vacuum. The dry, lipid film was rehydrated in Milli-Q water. Liposomes were formed during rotation at room temperature followed by 30 min sonication in an ultrasonic bath (USC300T, VWR, Radnor, PA, USA). The liposome suspension was passed 11x through a symmetric polycarbonate membrane with 200 nm pore size (Nuclepore; Whatman plc; Maidstone; UK) using a LiposoFast pneumatic extruder (Avestin, Ottawa, Canada).

Recrystallization of S-layer protein on liposomes

Liposomes and S-layer protein were mixed according to a DPPC to protein ratio of 1 mg : 2 mg in Milli-Q water. Recrystallization of the S-layer protein on the liposomes was carried out for 2 hours on a test tube rotator (Heidolph Reax 2, Germany) at 30 revelations per min at room temperature. Non reassembled protein was removed with the supernatant after centrifugation at 20 000 g for 10 min at room temperature [22].

Atomic force microscopy (AFM)

Imprinted and non-imprinted areas were investigated by AFM in contact and non-contact mode in buffer and also in air (Nanowizard I, JPK Berlin, Germany and Nanoscope V, Veeco, Santa Barbara, CA) [12, 32, 35]. Non-conductive silicon nitride cantilevers (Type DNP-S10, Bruker) were used in both microscopes.

Peak force QNM measurements

Peak Force Quantitative Nanomechanical Property Mapping (PF-QNM) was done with a MultiMode VIII Scanning Probe Microscope (Bruker, USA). Measurements in air were performed using a steel probe holder (MMEFCH, Bruker) with Scanasyst air cantilevers. Measurements in liquid with functionalized and non-functionalized tips were performed with a liquid electrochemistry tapping fluid cell (MMTMAC, Bruker) using Scanasyst fluid+ cantilevers. Spring constant values were obtained trough thermal tuning and the deflection sensitivity determined on glass. The nominal tip radius was verified by SEM. A Poisson ratio of 0.23 was assumed for the fitting procedure. Mean values and standard deviations (n=246) of adhesion forces were calculated from three different areas per sample (200 x 200 nm each). PF-QNM was performed with a scan rate of 0.2 Hz.

Tip functionalization

Scanasyst-fluid+ cantilever were treated in oxygen plasma (20 s at 0,01 mbar) (Model Plasma Prep II, Gala instruments, Germany) and subsequently immersed in 0.5 M NaOH, 0.1 M HCl, 0.5 M NaOH, 0.1 M HCl for 5 sec for each step and dried for 10 min. Afterwards, they were treated with 1H,1H,2H,2H- perfluorododecyltrichlososilane silizium nitride in order to obtain a very clean hydrophobic surface for the reassembly of the SbpA S-layer protein (0.1 mg/ mL SbpA in 0.5 mM Tris-HCl buffer, pH 9, 10 mM $CaCl_2$,, room temperature (RT)) over night (o.n.)). S-layer reassembly was carried out as described before for the preparation of the stamps. Blank reference tips were prepared in the same way but without the final S-layer reassembly. Spring constants and deflection sensitivities were rechecked as described before.

18 References

[1] Arshady R and Mosbach K 1981 Synthesis of substrate-selective polymers by host-guest polymerization *Die Makromolekulare Chemie* **182** 687-92

[2] Baranova E, Fronzes R, Garcia-Pino A, Van Gerven N, Papapostolou D, Pehau-Arnaudet G, Pardon E, Steyaert J, Howorka S and Remaut H 2012 SbsB structure and lattice reconstruction unveil Ca2+ triggered S-layer assembly *Nature* **487** 119-22

[3] Chung S, Shin S H, Bertozzi C R and De Yoreo J J 2010 Self-catalyzed growth of S layers via an amorphous-to-crystalline transition limited by folding kinetics *Proc. Natl. Acad. Sci. USA* **107** 16536-41

[4] Danon D, Skutelsk.E, Marikovs.Y and Goldstei.L 1972 Use of Cationized Ferritin as a Label of Negative Charges on Cell Surfaces *J Ultra Mol Struct R* **38** 500-&

[5] Dickert F L and Hayden O 2002 Bioimprinting of polymers and sol-gel phases. Selective detection of yeasts with imprinted polymers *Anal Chem* **74** 1302-6

[6] Dickert F L, Hayden O, Bindeus R, Mann K J, Blaas D and Waigmann E 2004 Bioimprinted QCM sensors for virus detection - screening of plant sap *Anal Bioanal Chem* **378** 1929-34

[7] Egelseer E, Leitner K, Jarosch M, Hotzy C, Zayni S, Sleytr U B and Sára M 1998 The S-layer proteins of two Bacillus stearothermophilus wild-type strains are bound via their N-terminal region to a secondary cell wall polymer of identical chemical composition *J Bacteriol* **180** 1488-95

[8] Egelseer E M, Ilk N, Pum D, Messner P, Schäffer C, Schuster B and Sleytr U B 2010 *Encyclopedia of industrial biotechnology: bioprocess, bioseparation, and cell technology,* ed M C Flickinger (Hoboken, N.J.: John Wiley and Sons) pp 4424-48

[9] Glad M, Norrlˆw O, Sellergren B, Siegbahn N and Mosbach K 1985 Use of silane monomers for molecular imprinting and enzyme entrapment in polysiloxane-coated porous silica *Journal of Chromatography A* **347** 11-23

[10] Göbel C, Schuster B, Baurecht D, Sleytr U B and Pum D 2010 S-layer templated bioinspired synthesis of silica *Coll. Surf. B* **75** 565-72

[11] Györvary E, Schroedter A, Talapin D V, Weller H, Pum D and Sleytr U B 2004 Formation of nanoparticle arrays on S-layer protein lattices *J. Nanosci. Nanotech.* **4** 115-20

[12] Györvary E S, Stein O, Pum D and Sleytr U B 2003 Self-assembly and recrystallization of bacterial S-layer proteins at silicon supports imaged in real time by atomic force microscopy *J. Microsc.* **212** 300-6

[13] Hayden O and Dickert F L 2001 Selective microorganism detection with cell surface imprinted polymers *Adv Mater* **13** 1480-+

[14] Horejs C, Gollner H, Pum H, Sleytr U B, Peterlik H, Jungbauer A and Tscheliessnig R 2011 Atomistic structure of monomolecular surface layer self-assemblies: toward functionalized nanostructures *ACS Nano* **5** 2288-97

[15] Horejs C, Pum D, Sleytr U B and Tscheliessnig R 2008 Structure prediction of an S-layer protein by the mean force method *J. Chem. Phys.* **128** 65106

[16] Ilk N, Egelseer E M, Ferner-Ortner J, Küpcü S, Pum D, Schuster B and Sleytr U B 2008 Surfaces functionalized with self-assembling S-layer fusion proteins for nanobiotechnological applications *Coll. Surf. A* **321** 163-7

[17] Ilk N, Egelseer E M and Sleytr U B 2011 S-layer fusion proteins - construction principles and applications *Curr. Opin. Biotechnol.* **22** 824-31

[18] Ilk N, Kosma P, Puchberger M, Egelseer E M, Mayer H F, Sleytr U B and Sára M 1999 Structural and functional analyses of the secondary cell wall polymer of Bacillus sphaericus CCM 2177 that serves as an S-layer-specific anchor *J. Bacteriol.* **181** 7643-6

[19] Ilk N, Völlenkle C, Egelseer E M, Breitwieser A, Sleytr U B and Sára M 2002 Molecular characterization of the S-layer Gene, sbpA, of Bacillus sphaericus CCM 2177 and production of a functional S-layer fusion protein with the ability to recrystallize in a defined orientation while presenting the fused allergen *Appl. Environ. Microbiol.* **68** 3251-60

[20] Kirby C and Gregoriadis G 1984 Dehydration-Rehydration Vesicles - a Simple Method for High-Yield Drug Entrapment in Liposomes *Bio-Technol* **2** 979-84

[21] Latif U, Can S, Hayden O, Grillberger P and Dickert F L 2013 Sauerbrey and anti-Sauerbrey behavioral studies in QCM sensors-Detection of bioanalytes *Sensor Actuat B-Chem* **176** 825-30

[22] Mader C, Küpcü S, Sleytr U B and Sára M 2000 S-layer-coated liposomes as a versatile system for entrapping and binding target molecules *Biochim. Biophys. Acta* **1463** 142-50

[23] Martín-Molina A, Moreno-Flores S, Perez E, Pum D, Sleytr U B and Toca-Herrera J L 2006 Structure, surface interactions, and compressibility of bacterial S-layers through scanning force microscopy and the surface force apparatus *Biophys. J.* **90** 1821-9

[24] Messner P, Pum D, Sára M, Stetter K O and Sleytr U B 1986 Ultrastructure of the cell envelope of the archaebacteria *Thermoproteus tenax* and *Thermoproteus neutrophilus J. Bacteriol.* **166** 1046-54

[25] Messner P, Schaffer C and Kosma P 2013 Bacterial cell-envelope glycoconjugates *Advances in carbohydrate chemistry and biochemistry* **69** 209-72

[26] Moll D, Huber C, Schlegel B, Pum D, Sleytr U B and Sára M 2002 S-layer-streptavidin fusion proteins as template for nanopatterned molecular arrays *Proc. Natl. Acad. Sci. USA* **99** 14646-51

[27] Norville J E, Kelly D F, Knight T F, Belcher A M and Walz T 2007 7Å projection map of the S-layer protein sbpA obtained with trehalose-embedded monolayer crystals *J. Struct. Biol.* **160** 313-23

[28] Pavkov-Keller T, Howorka S and Keller W 2011 The structure of bacterial S-layer proteins *Prog. Molec. Biol. Transl. Sci.* **103** 73-130

[29] Pum D, Sára M and Sleytr U B 1989 Structure, surface charge and self-assembly of the S-layer lattice from Bacillus coagulans E38-66 *J. Bacteriol.* **171** 5296-303

[30] Pum D and Sleytr U B 1994 Large-scale reconstruction of crystalline bacterial surface layer proteins at the air-water interface and on lipids *Thin Solid Films* **244** 882-6

[31] Pum D and Sleytr U B 1995 Anisotropic crystal growth of the S-layer of Bacillus sphaericus CCM 2177 at the air/water interface *Coll. Surf. A* **102** 99-104

[32] Pum D and Sleytr U B 1995 Monomolecular reassembly of a crystalline bacterial cell surface layer (S-layer) on untreated and modified silicon surfaces *Supramol. Sci.* **2** 193-7

[33] Pum D and Sleytr U B 2014 Reassembly of S-layer proteins *Nanotechnology* **25** 312001

[34] Pum D, Stangl G, Sponer C, Fallmann W and Sleytr U B 1997 Deep UV patterning of monolayers of crystalline S layer protein on silicon surfaces *Coll. Surf. B* **8** 157-62

[35] Pum D, Tang J, Hinterdorfer P, Toca-Herrera J L and Sleytr U B 2010 *Biomimetic and bioinspired nanomaterials,* ed C Kumar (Weinheim: Wiley-VCH) pp 459-510

[36] Rad B, Haxton T K, Shon A, Shin S-H, Whitelam S and Ajo-Franklin C M 2014 Ion-Specific Control of the Self-Assembly Dynamics of a Nanostructured Protein Lattice *ACS Nano*

[37] Rünzler D, Huber C, Moll D, Kohler G and Sara M 2004 Biophysical characterization of the entire bacterial surface layer protein SbsB and its two distinct functional domains *The Journal of biological chemistry* **279** 5207-15

[38] Sára M, Dekitsch C, Mayer H F, Egelseer E M and Sleytr U B 1998 Influence of the secondary cell wall polymer on the reassembly, recrystallization, and stability properties of the S-layer protein from Bacillus stearothermophilus PV72/p2 *J. Bacteriol.* **180** 4146-53

[39] Sára M, Kuen B, Mayer H F, Mandl F, Schuster K C and Sleytr U B 1996 Dynamics in oxygen-induced changes in S-layer protein synthesis from *Bacillus stearothermophilus* PV72 and the S-layer-deficient variant T5 in continuous culture and studies of the cell wall composition *J Bacteriol* **178** 2108-17

[40] Schirhagl R, Lieberzeit P A and Dickert F L 2010 Chemosensors for Viruses Based on Artificial Immunoglobulin Copies (vol 22, pg 2078, 2010) *Adv Mater* **22** 1992-

[41] Schuster B and Sleytr U B 2015 Relevance of glycosylation of S-layer proteins for cell surface properties *Acta Biomater* **19** 149-57

[42] Schuster D, Küpcü S, Belton D J, Perry C C, Stöger-Pollach M, Sleytr U B and Pum D 2013 Construction of silica enhanced S-layer protein cages *Acta Biomaterialia* **9** 5689-97

[43] Shenton W, Pum D, Sleytr U B and Mann S 1997 Biocrystal templating of CdS superlattices using self-assembled bacterial S-layers *Nature* **389** 585-7

[44] Shin S H, Chung S, Sanii B, Comolli L R, Bertozzi C R and De Yoreo J J 2012 Direct observation of kinetic traps associated with structural transformations leading to multiple pathways of S-layer assembly *Proc. Natl. Acad. Sci. USA* **109** 12968-73

[45] Sleytr U B 1970 Fracture Faces in Intact Cells and Protoplasts of Bacillus-Stearothermophilus - Study by Conventional Freeze-Etching and Freeze-Etching of Corresponding Fracture Moieties *Protoplasma* **71** 295-&

[46] Sleytr U B, Messner P, Pum D and Sára M 1999 Crystalline bacterial cell surface layers (S layers): From supramolecular cell structure to biomimetics and nanotechnology [Review] *Angew. Chem. Int. Ed.* **38** 1035-54

[47] Sleytr U B and Robards A W 1977 Plastic-Deformation during Freeze-Cleavage - Review *J Microsc-Oxford* **110** 1-25

[48] Sleytr U B and Robards A W 1982 Understanding the Artifact Problem in Freeze-Fracture Replication - a Review *J Microsc-Oxford* **126** 101-22

[49] Sleytr U B, Sára M, Küpcü Z and Messner P 1986 Structural and chemical characterization of S-layers of selected strains of Bacillus stearothermophilus and Desulfotomaculum nigrificans *Archives of Microbiology* **146** 19-24

[50] Sleytr U B, Schuster B, Egelseer E M and Pum D 2014 S-layers: principles and applications *FEMS Microbiol Rev* **38** 823-64

[51] Sleytr U B and Umrath W 1974 Simple Fracturing Device for Obtaining Complementary Replicas of Freeze-Fractured and Freeze-Etched Suspensions and Tissue Fragments *J Microsc-Oxford* **101** 177-86

[52] Tschiggerl H, Casey J L, Parisi K, Foley M and Sleytr U B 2008 Display of a peptide mimotope on a crystalline bacterial cell surface layer (S-layer) lattice for diagnosis of Epstein-Barr virus infection *Bioconj. Chem.* **19** 860-5

[53] Turner N W, Jeans C W, Brain K R, Allender C J, Hlady V and Britt D W 2006 From 3D to 2D: a review of the molecular imprinting of proteins *Biotechnol Prog* **22** 1474-89

[54] Wangchareansak T, Sangma C, Choowongkomon K, Dickert F and Lieberzeit P 2011 Surface molecular imprints of WGA lectin as artificial receptors for mass-sensitive binding studies *Anal Bioanal Chem* **400** 2499-506

1.

1. Report Type

Final Report

Primary Contact E-mail
Contact email if there is a problem with the report.

dietmar.pum@boku.ac.at

Primary Contact Phone Number
Contact phone number if there is a problem with the report

+431476542205

Organization / Institution name

Department fuer Nanobiotechnologie

Grant/Contract Title
The full title of the funded effort.

S-layer based bio-imprinting - Synthetic S-layer polymers

Grant/Contract Number
AFOSR assigned control number. It must begin with "FA9550" or "F49620" or "FA2386".

FA9550-12-1-0274

Principal Investigator Name
The full name of the principal investigator on the grant or contract.

Prof. Dietmar Pum

Program Manager
The AFOSR Program Manager currently assigned to the award

Dr. Hugh C. De Long

Reporting Period Start Date

06/01/2012

Reporting Period End Date

05/31/2015

Abstract

The main objective of the proposed work is the development of a key enabling technology for the fabrication of nano patterned thin film imprints by using functional S-layer protein arrays as templates. The unique feature of these imprints is the precisely controlled repetition of surface functional groups and topographical features – induced by the crystalline character of the reassembled S-layer protein lattice.

According to the project plan, work continued with the investigation of imprinting spherical S-layer architectures. Micrometer sized liposomes or silica spheres offer the advantage of increased surface areas and consequently a higher number of functional groups or domains. Unfortunately, those experiments did not yield the expected results since liposomes were not stable in DMSO (dimetylsulfoxide) that is used in the polymer synthesis and silica particles were completely enclosed by the polymer and subsequently could not be removed from the imprint. Nevertheless, in the course of theses experiments, S-layer coated bacterial cells (L. sphaericus CCM2177) were successfully used as templates. Atomic Force Microscopy (AFM) demonstrated the successful imprinting of the bacterial cells and the attached S-layer lattice.

However, despite the initial assumption, it was not possible to resolve the imprinted S-layer lattice by AFM. We assume that several factors are responsible for this such as plastic deformation at molecular level upon

removing the template, water cushions between the S-layer template and the polymer preventing a successful transfer of the S-layer topography into the polymer, or too shallow surface corrugations in relation to the roughness of the polymer. However, Peak Force Quanto Nanomechanical property Mapping (PF-QNM) was able to show that the adhesion of an S-layer coated AFM-tip at the (blank) S-layer imprint was significantly higher than that at the blank reference area.

In summary, we would like to anticipate that our approach provides a key enabling technology for the fabrication of nano patterned molecular imprints by using self-assembled S-layer lattices. Applications will be found in the life and non-life sciences wherever well defined repetitive topographic and (bio)chemical features in the nanometer range are required.

Distribution Statement

This is block 12 on the SF298 form.

Distribution A - Approved for Public Release

Explanation for Distribution Statement

If this is not approved for public release, please provide a short explanation. E.g., contains proprietary information.

SF298 Form

Please attach your SF298 form. A blank SF298 can be found here. Please do not password protect or secure the PDF The maximum file size for an SF298 is 50MB.

SF298.pdf

Upload the Report Document. File must be a PDF. Please do not password protect or secure the PDF . The maximum file size for the Report Document is 50MB.

Final Report SLI.pdf

Upload a Report Document, if any. The maximum file size for the Report Document is 50MB.

Archival Publications (published) during reporting period:

1. Zafiu, C., Werzer, T., Trettenhahn, G., Pum, D., Sleytr, U.B., Kautek, W. 2014. In Situ Scanning Force Microscopy and In Situ Quartz Microbalance Investigations on the Influence of the Anion Adsorption on the Electrocrystallization of Surface Layer Proteins. J. Phys. Chem. C 118 29860-29865.

2. Pum, D., Sleytr, U.B. 2014. Reassembly of S-layer proteins. Nanotechnology 25:312001.

3. Sleytr, U.B., Schuster, B., Egelseer, E.M., Pum, D. S-layers: Principles and Applications. FEMS Microbiology Review 38:823-864.

4. Prats Mateu, B. Kainz, B., Pum, D., Sleytr, U.B., Toca-Herrera, J.L. 2014. Fluorescent sensors based on bacterial fusion proteins. Methods and Applications in Fluorescence 2:024002

5. Gahleitner, B., Loderer, C., Saracino, C., Pum, D., Fuchs, W. 2014. Chemical foam cleaning as an efficient alternative for flux recovery in ultrafiltration processes. J. Membrane Sci. 450:433-439.

6. Sekot, G. Schuster, D., Messner, P., Pum, D. Peterlik, H., Schäffer, C. SAXS for imaging of S-layers on intact bacteria in the native environment. J. Bacteriol. 195:2408-2414.

7. Pum, D., Toca-Herrera, J.L., Sleytr, U.B. 2013. S-layer protein self-assembly. Int. J. Mol. Sci. 14:2484-2501

8. Schuster, D., Küpcü, S., Belton, D. J., Perry, C. C., Stöger-Pollach, M., Sleytr, U.B., Pum, D., 2013. Construction of silica enhanced S-layer protein cages. Acta Biomaterialia 9:5689-5697

Changes in research objectives (if any):

Change in AFOSR Program Manager, if any:

Extensions granted or milestones slipped, if any:

AFOSR LRIR Number

LRIR Title

Reporting Period

Laboratory Task Manager

Program Officer

Research Objectives

Technical Summary

Funding Summary by Cost Category (by FY, $K)

	Starting FY	FY+1	FY+2
Salary			
Equipment/Facilities			
Supplies			
Total			

Report Document

Report Document - Text Analysis

Report Document - Text Analysis

Appendix Documents

2. Thank You

E-mail user

Jul 06, 2015 05:08:37 Success: Email Sent to: dietmar.pum@boku.ac.at